Analytical Methods

Accepted Manuscript

This article can be cited before page numbers have been issued, to do this please use: A. Joorab Doozha and K. Poduska, *Anal. Methods*, 2019, DOI: 10.1039/C9AY00046A.

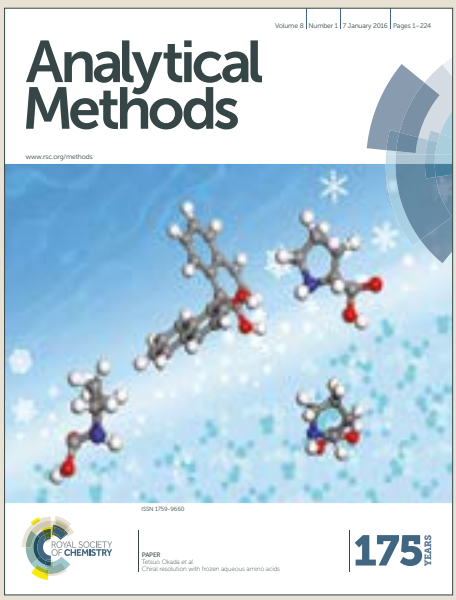

ROYAL SOCIETY OF CHEMISTRY

rsc.li/methods

View Article Online
DOI: 10.1039/C9AY00046A

Journal Name

ARTICLE TYPE

Cite this: DOI: 10.1039/xxxxxxxxxx

Graphite oxidation chemistry is relevant for designing cleaning strategies for radiocarbon dating samples†

Amir Joorab Doozha[a] and Kristin M. Poduska*[,a,b]

Received Date
Accepted Date

DOI: 10.1039/xxxxxxxxxx

www.rsc.org/journalname

We demonstrate that mixtures of graphite and lab-oxidized graphenic carbon materials can be separated into three individual components (graphite, graphene/graphite oxide (GO) and oxidative debris (OD)) by a series of aqueous treatments. Our results show that a key part of this separation procedure involves a water treatment and sonication near neutral pH in order to separate GO from OD. We show that the relative proportions of OD and GO – independent of any humic substances – can affect the ability of oxidized graphite to be suspended in water, which can influence the efficiency of the separation procedures we describe. We compare and contrast our protocol with others that are widely used for cleaning archaeological charcoal prior to radiocarbon dating. Our protocol has potential applications for tailored cleaning procedures for graphenic carbon materials, including the possibility of separating GO from both OD and from graphite, for radiocarbon dating purposes.

1 Introduction

Graphenic carbon material from archaeological samples is widely used for radiocarbon (^{14}C) dating.[1–3] However, datable material must be cleaned to remove carbonaceous contaminants that contribute to specimen radiocarbon levels. Because different forms of carbon-containing materials have very different chemistry, there are specialized decontamination procedures for minerals (such as bone), organic materials (such as collagen), and graphenic materials (such as charcoal). An extremely effective cleaning method – that applies uniquely to graphenic carbon materials – involves a successive acid-base-acid (ABA) treatment,[4] as shown schematically in Figure 1a. Previous studies have concluded that the first concentrated acid rinse expands the spacing between graphitic layers to remove intercalated counterions[5,6] and mineralized carbonates,[2] washing with concentrated base remove humic substances,[1,2,4] and the last concentrated acid wash removes surface-adsorbed CO_2.[2] Samples are exposed to water between each step to rinse and neutralize pH. Although the ABA cleaning method is used routinely in radiocarbon laboratories throughout the world, poorly preserved specimens can be completely broken down during the water and base rinses, thereby leaving no solid material for dating. To address this problem, it is an ongoing area of research to investigate modifications and alternatives to the ABA cleaning treatment that can be tailored for poorly preserved specimens.[2,3,7,8]

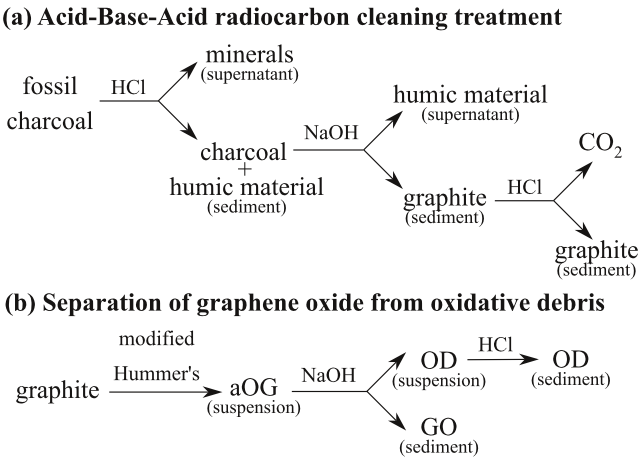

Fig. 1 Schematic comparisons between (a) typical acid-base-acid (ABA) cleaning for radiocarbon samples and (b) steps to separate graphene oxide (GO) and oxidative debris (OD) from as-prepared oxidized graphite (aOG). All HCl and NaOH treatments are at 1 M.

The radiocarbon ABA treatment steps resemble the series of base and acid treatments that are typically involved in producing graphene oxide from graphite. Graphite oxidation has drawn a great deal of attention from chemists since it improves the ability to suspend graphenic carbon materials in water.[9,10] However, the oxidation processes tend to yield graphenic particles with a range of different lateral dimensions, thicknesses, oxidation lev-

[a] Department of Chemistry, Memorial University of Newfoundland, St. John's, Canada.
[b] Department of Physics and Physical Oceanography, Memorial University of Newfoundland, St. John's, Canada. Fax: +1 709 864-8739; Tel: +1 709 864-8890; E-mail: kris@mun.ca

† Electronic Supplementary Information (ESI) available: [details of any supplementary information available should be included here]. See DOI: 10.1039/b000000x/

View Article Online
DOI: 10.1039/C9AY00046A

els, and surface terminations.[11,12] For clarity, in this work we adopt nomenclature for different kinds of graphenic carbon particles that was put forward by others.[13]

One of the most efficient ways to oxidize graphite is by chemical methods,[14,15] as shown schematically in Figure 1b. As-prepared oxidized graphite (aOG) is readily suspended in water, and it has been shown to consist of a combination of graphene oxide (GO) along with highly oxidized, low molecular weight oxidative debris (OD).[16,17] In order to separate GO from OD, the as-prepared product can be treated with concentrated base causing the GO to sediment while the OD remains in the supernatant.[10,17] OD can then be precipitated from the supernatant using concentrated acid.[10,17]

Despite the similarities between the radiocarbon ABA cleaning procedure and the GO isolation procedure, there is virtually no overlap between these two fields in the literature. It is well documented that the ABA protocol separates humic substances, which are highly oxidized carbonaceous species, from graphite.[1,2,4] Previous radiocarbon-related literature shows evidence that oxidized graphite exists in archaeological charcoal.[18] GO-related literature is more recent, and some reports equate OD with humic substances.[10,19] However, no studies have investigated how graphenic carbon material that is intentionally oxidized is affected during different steps of the ABA cleaning procedure.

In this work, we show that there are synergies between (1) the chemistry involved in removing OD and GO from aOG and (2) the chemistry involved in the ABA cleaning of graphenic carbon materials used for radiocarbon dating. First, we show that a different cleaning sequence of water/sonication-base-acid (WSBA) helps to separate oxidized graphite from graphite and oxidative debris. Next, we use existing knowledge of OD chemistry to explain why water and base rinses could diminish the quantity of graphenic carbon material that can be recovered after a standard ABA treatment. Finally, we demonstrate that the relative proportions of OD and aOG – independent of any humic substances – can affect the ability of oxidized graphite to be suspended in water, which can affect the efficiency of such separation procedures.

2 Experimental

2.1 Oxidation of graphenic carbon materials

Starting materials were graphite flakes (Alfa Aesar, 99.8% purity, 325 mesh) or pyrolyzed charcoal (mixture of fir and pine, heated in a nitrogen atmosphere from 30°C to 480°C over 1 hour, then held at 480°C for 20 minutes). All purchased chemicals were ACS reagent grade: $KMnO_4$ (99%), NaOH (97%), and H_2O_2 (30%) from ACP, with HCl (38%) from Caledon, and H_2SO_4 (98%) from Merck. All reactions used ultrapure water (Barnstead Nanopure Diamond, 18.2 MΩ·cm).

Our graphite oxidization protocol followed a modified Hummer's method.[20,21] Powdered graphite or charcoal (1 g) was stirred in 50 mL H_2SO_4 for 1 hour while immersed in an ice bath to hold the temperature at 0 °C. Then, 3 g of $KMnO_4$ was added very slowly over 1 hour while keeping the temperature between 0 and 5 °C. The mixtures were then removed from the ice bath and warmed to room temperature during continuous stirring. After an hour, the mixtures became very thick and difficult to stir. They were then heated to 40 °C and left for 1 hour under automatic stirring (800 rpm). 80 mL of nanopure water was then added to the mixtures over a span of 5 minutes, after which the temperature was increased to 90 °C, followed by stirring for another hour. Afterwards, 6 mL H_2O_2 was added to the mixtures along with 200 mL water, followed by 1 hour of stirring. At this point, the product from graphite flakes transformed into a golden suspension, while the product from charcoal became an opaque dark brown suspension. The mixtures were centrifuged at 8500 rpm for 10 minutes to separate the sediment from the supernatant. The sediments were washed 3 times with nanopure water, yielding either a brown jelly (when derived from graphite flakes) or a dark brown sludge (when derived from charcoal). Sediments were dried in an oven overnight at 50 °C. In the remainder of this work, we refer to these dried sediments as either as-prepared oxidized flake graphite (aOG) or as-prepared oxidized charcoal (aOC).

2.2 Isolating GO and OD from oxidized graphenic carbon materials

Sequential base and acid treatments facilitated separation of graphite/graphene oxide (GO) and oxidative debris (OD) from aOG and aOC.[10,17]

0.05 g of brown aOG solid (or black aOC solid) was dispersed in 250 mL of 1 M NaOH and stirred for 1 hour under reflux conditions at 90 °C. Immediately after adding base, the aOG mixture became dark and opaque; the aOC became transparent light brown. After the coagulants cooled to room temperature, centrifugation separated the black solid residuals from the supernatants. The supernatant from aOG was clear and colourless, while the aOC supernatant was transparent light brown. The solid residuals were dispersed in water and centrifuged; after 5 such rinses, the supernatant had neutral pH. The resulting sediment was GO, and the supernatant contained OD in suspension.

250 mL of 1 M HCl was added to the OD-containing supernatants obtained after both base washing and neutralization, followed by 30 min of stirring and oven-drying at 60 °C overnight. The powder that remained was OD (white from the aOG precursor, and pale yellow from the aOC precursor).

2.3 Specimen characterization

Attenuated total reflectance Fourier transform infrared (ATR-FTIR) spectra were recorded using a Bruker Alpha II spectrometer (diamond crystal, 36 scans, 4 cm^{-1} resolution). UV-VIS spectra were acquired with a Varian Cary 6000 spectrometer with 0.1 second average time, 1 nm resolution, and 600 nm/min scan rate. Representative particle sizes were assessed from optical microscopy images (Leica, 5x and 20x NPLAN objectives) that were analyzed using Fiji particle analysis routines.[22]

View Article Online
DOI: 10.1039/C9AY00046A

3 Results and discussion

3.1 Separating mixtures with WSBA

In an archaeological charcoal sample, one might expect to find a mixture of graphite, GO, and OD, along with other foreign material. As a simpler test case, we outline a protocol to separate a mixture of graphite, aOG, and OD. This water/sonication-base-acid (WSBA) procedure is shown schematically in Figure 2, and summarized in Table 1.

Action	Description
0. Starting mixture	graphite (0.02 g) + aOG (0.02 g) + nanopure water (10 mL)
1. Sonication	60 minutes
2. Filtration	8 μm pore size paper (Whatman)
3. Dry solid (1), retain	8-12 hours at 50 °C
4. Base treat the filtrate	1 M NaOH (pH=13, 20 mL) for 1 hour at 100 °C
5. Filtration	8 μm filter paper (Whatman)
6. Dry solid (2), retain	8-12 hours at 40 °C
7. Acidify the filtrate	1 M HCl (pH=2, 20 mL)
8. Dry solid (3), retain	12 hours at 80 °C

Table 1 A summary of the water/sonication-base-acid separation protocol. This produces three different solids: (1) as-prepared oxidized graphite (aOG), (2) graphite/graphene oxide (GO), and (3) oxidative debris (OD).

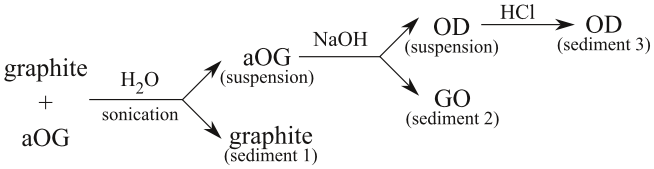

Fig. 2 Water/sonication-base-acid (WSBA) protocol for separating GO (sediment 2) from graphite (sediment 1) and OD (sediment 3).

Infrared spectroscopy allowed us to track structural changes in individual components, and also provided a qualitative way to monitor the efficacy and range of product variability at each separation step. Figure 3 compares ATR-FTIR spectra for each component at different stages of the WSBA procedure, displaying representative spectra from three different separation experiments using the same starting materials. These spectra are discussed below in the context of each stage of the separation protocol.

The first step in our WSBA protocol is sonication in water. Others report that, during sonication, aOG breaks into smaller pieces more easily than graphite breaks.[23,24] There is a strong precedent in the literature for using sonication to alter the size of oxidized graphenic carbon.[25–27] We exploit this to separate the larger graphite pieces from the smaller aOG pieces by filtration (Step 2 in Table 1).

Our IR data suggest that this combination of sonication and filtration works very well to extract graphite. Reports by others[28,29] show that graphite flakes do not exhibit many distinguishable IR peaks, and our data (Figure 3a) is consistent with this. Weak absorption bands at 3400 and 1600 cm^{-1} are due to O-H stretches

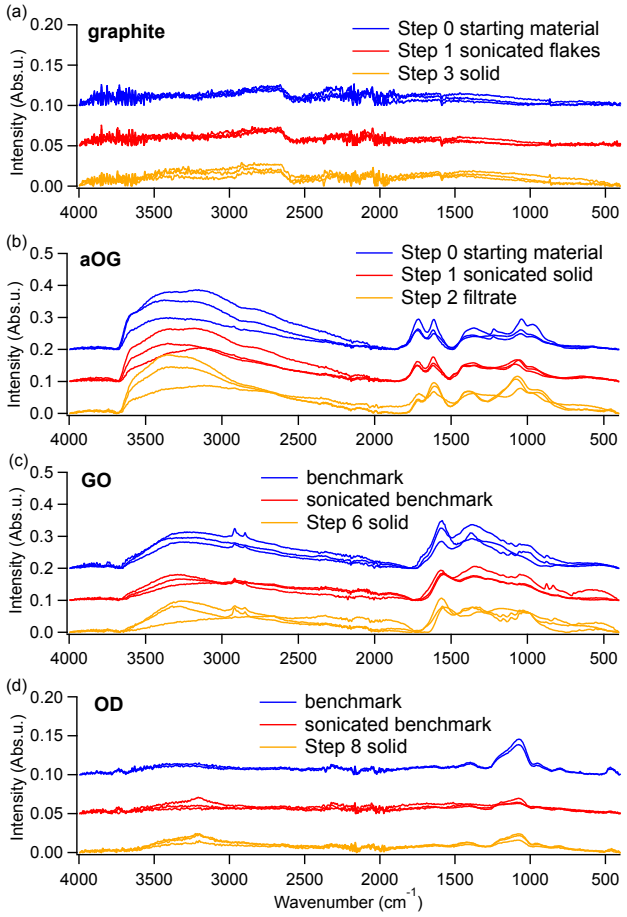

Fig. 3 Representative ATR-FTIR spectra, before (blue) and after (red) sonication in water, of (a) graphite flakes, (b) aOG, (c) GO and (d) OD. Spectra are offset along the vertical axis for clarity. In each plot, the orange spectra correspond to the extracted component after the noted WSBA step. The plot legends indicate the precise preparation conditions for each sample, based on the procedure outlined in Table 1. In (c) and (d), the benchmark GO and OD samples were separated from unsonicated aOG using 1 M NaOH (pH=13) followed by 1 M HCl (pH=2). Note that the intensity scales for (a) and (d) are the same, and that they are expanded relative to (b) and (c).

and C=C vibrations, respectively.[29] Figure 3a shows that there is no change in the IR peak positions between the starting graphite flakes (blue spectra) and the graphite after sonication (red spectra). Furthermore, the sonicated, large-size-filtered solid (orange spectra) does not show any additional peaks in the IR spectrum.

Unlike graphite, the aOG that exists in the filtrate (Step 2 in Table 1) shows very distinctive IR peaks (Figure 3b) due to the formation of oxygen-related functional groups such as carboxyl, alcohol, epoxide, and carbonyl. The peak positions for our aOG specimens are consistent with results from others.[17,20,21,30] The peaks at 2800 and 2900 cm^{-1} are due to CH_2 symmetric and asymmetric stretching modes, respectively. The peak at 1600 cm^{-1} is associated with water bending, while the 1300 cm^{-1} peak results from C-O stretches. The broad band from 2400 to 3800 cm^{-1} is related to O-H stretching modes, the sharp peak near 1700 cm^{-1} is associated with carbonyl groups, and the peak near 1030 cm^{-1} is related to C-O bonds in ester and carboxylic acid.

View Article Online
DOI: 10.1039/C9AY00046A

Others have shown that size of GO flakes, and thus changes to the edge-to-area ratio, will affect the relative proportion of edge-groups (COOH) and in-sheet defects (C-O), which contributes to variations in relative FTIR peak intensities.[26,27] Indeed, we observed changes in FTIR relative peak intensities before and after sonication. We note that we cannot rule out the possibility that some smaller graphite pieces exist and remain mixed with the aOG in the Step 2 filtrate. Similarly, it is possible that a small amount of aOG remains attached to the the filter paper.

Once the graphite solid is removed, the filtrate is then treated with strong base (Step 4 in Table 1) to dissociate GO (which is larger and less hydrophilic) from OD (which is smaller and tends to remain in suspension).[10,17,31] We note that these experimental conditions (NaOH at pH 11 and 25 °C) are not strong enough to trigger any reduction processes, and merely serves to decouple aOG into its two components: GO and OD. Figure 3c shows that GO obtained after base treatment, filtration and drying (Steps 4, 5, 6 in Table 1) has similar IR peak positions and relative intensities whether with or without exposure to sonication. The peak intensity variations that occur in the fingerprint region between 1000 and 1300 cm^{-1} vary from work to work and from sample to sample, regardless of exposure to sonication.[12,16,17,20] The vibrational modes that contribute to peaks in this region are difficult to identify definitively because different oxygen-based functional groups contribute to many overlapping peaks. However, a typical FTIR spectrum for GO shows a broad peak near 3400-3700 cm^{-1} for O-H stretching, a peak near 1720 cm^{-1} due to carbonyl vibrations, another peak near 1600 cm^{-1} for water bending modes, and a peak near 1040 cm^{-1} for C-O. We note that peaks at 2800 and 2900 cm^{-1} are associated with symmetric and asymmetric stretching modes[32] of CH_2 and have been reported in GO samples,[33–35] but could be influenced by sonication.[36]

To extract the remaining solid component (OD), the filtrate is acidified and dried (Steps 7, 8 in Table 1) by using chemistry that is well documented in the literature.[10,17,31] Figure 3d shows that IR spectra of OD are similar with or without exposure to sonication. Oxidized functional groups (C-OH and O-H) can cause the sharp peaks at 1100 and 3200 cm^{-1} for OD.[10,37]

We note that filter paper alone is not sufficient to separate GO from OD; both will pass through filter paper. OD (like GO) has a variable chemical composition and size. It is well documented in the literature that the main difference between them is that OD is smaller and more highly oxidized than GO. It is also well established that in neutral and alkaline solutions, OD complexes with GO. When aOG is added to a highly alkaline solution, it dissociates into its two constituents: the GO sediments, while the OD remains suspended.

As an overall comparison of the WSBA protocol, Figure 4a compares IR spectra for the starting mixture (Step 0) with spectra for the three extracted solids: graphite, GO, and OD (from Steps 3, 6, and 8, respectively). It is noteworthy that the sum of the three spectra for the extracted solids would not be identical to spectra for the starting mixture. One of the most obvious discrepancies occurs in the range of 1500-1700 cm^{-1} (Figure 4a), where a definitive GO peak does not align with any spectral features from the starting mixture. There are several contributing factors to these discrepancies.

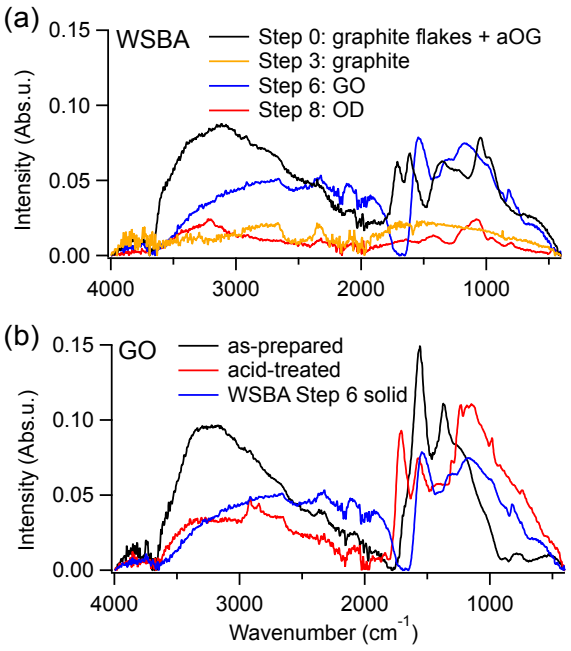

Fig. 4 (a) Representative ATR-FTIR spectra for solids extracted at different stages of the WSBA protocol: starting mixture (black), graphite from Step 3 (orange), GO from Step 6 (blue), and OD from Step 8 (red). (b) Representative ATR-FTIR spectra of GO before and after acid treatment.

First, the pH history of GO affects its IR spectrum. Figure 4b shows that there are many changes to peak positions and relative intensities after GO is exposed to different pH conditions (while in aqueous suspension) and then dried. After exposure to 1 M NaOH, GO peaks near 1600 and 1400 cm^{-1} increase, while spectral features near 1700 cm^{-1} decrease. The relative peak intensities reverse after exposure to 1 M HCl. Such pH-dependent changes have been noted by others who monitored the IR spectra of charcoal after ABA treatments,[2] and also by others investigating water-GO interactions.[12] Interpreting these pH-dependent peak intensity changes is surprisingly complex. For graphenic carbon materials, IR peaks have been attributed to carbonyl vibrations[12] (near 1700 cm^{-1}), C=C vibrations[29,38,39] (near 1600 cm^{-1}), and stretching modes of COO^- or C-OH (near 1400 and 1200 cm^{-1}).[2,39] However, a bending mode of water also occurs in this region[11,12,40] (1609 cm^{-1}), as do S=O stretching modes.[30] In our case, it is possible that sulfates were introduced at epoxide groups[30] while in the presence of H_2SO_4 during the initial preparation of the oxidized graphite starting material.

If one naively assumes that changes in relative IR peak intensities near 1600 cm^{-1} are affected solely by the relative number of these different chemical moieties, then one might conclude from Figure 4b that a pH increase removes carbonyl groups and increases water, COO^-, C-OH, or S=O groups. However, detailed studies by others[12] that correlated IR spectra with NMR in isotopically altered samples suggest that such changes are likely caused by IR absorbance differences of water due to reorientation in the presence of Na^+. Thus, even though the changes in rela-

View Article Online
DOI: 10.1039/C9AY00046A

tive IR peak intensities are consistent across different specimens and are clearly correlated with the sample's pH history, it is not appropriate to infer detailed structural information from IR peak intensity changes alone.

3.2 Interactions between GO and OD in water

Since the WSBA separation procedure relies on separating components by sedimentation, there is the potential to fine tune the separation procedure if one can change the amount or stability of material in suspension. We show that the relative quantity of OD plays an important role in the ability of aOG to remain suspended in water over time.

For context, previous studies have shown that chemical oxidization produces GO and OD in 2:1 ratio, and that OD adheres to GO by hydrogen bonding to making the as-prepared complex easy to suspend in water.[10] Because both OD and GO react readily with water and can exist in a range of sizes, there is no fixed chemical structure or composition for either OD or GO.[16]

In our experiments with enriched OD levels, 0.03 g of aOG was dispersed in 50 mL of nanopure water, then divided into 15 mL aliquots, with 0.5 g of OD added (extracted from either aOG or aOC). These mixtures, along with a control sample containing only aOG, were stirred at 400 rpm for 15 minutes and then left standing for one day.

Figure 5 shows different time-dependent sedimentation behavior with and without enriched OD levels. After one day, an aOG suspension (Figure 5a) shows a dark opaque sediment that is clearly separated from a translucent brown supernatant. Under the same conditions, the presence of additional OD (Figure 5b) causes a uniformly coloured translucent suspension with no visible sediment. Based on these results, it is tempting to assume that additional OD makes aOG more soluble in water. However, lengthening the sedimentation time to 7 days (Figure 5c,d) demonstrates that OD does not dissolve aOG, but instead helps it to aggregate and precipitate out over time. To help support this conclusion, representative UV-vis spectra for these different supernatants are compared in Figure 5e. The aOG (solid black curve) has a distinctive peak near 220 nm and a shoulder near 300 nm, which others have attributed to different electronic transitions within graphenic carbon materials.[15,20] These characteristic spectral features appear in supernatants from unenriched aOG after 1 day (solid blue curve) and 7 days (dashed blue curve), as well as in OD-enriched mixtures after 1 day (solid red curve). However, supernatant from OD-enriched mixtures after 7 days (dashed red curve) have no distinctive UV-vis features, which is consistent with the absence of aOG in the supernatant.[31]

This simple enrichment experiment is important for several reasons. First, our results demonstrate that the relative proportions of OD and aOG – independent of any humic substances – can affect how readily oxidized graphite stays in suspension over time. This means that time and OD enrichment protocols could – in principle – be developed to help separate graphite from OD and GO.

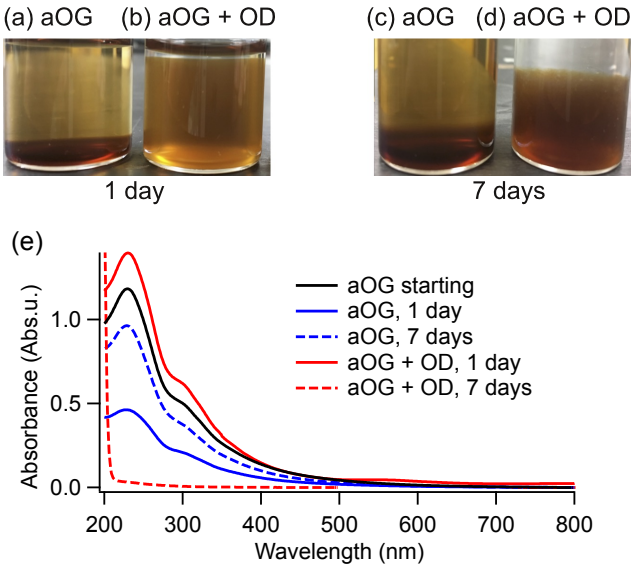

Fig. 5 Photographs of aOG (a,c) and aOG + extra OD (b,d) after one day (a,b) and seven days (c,d). Plot (e) compares representative UV spectra of fresh aOG suspension (black curve) with supernatants of aOG (blue curves) and OD-enriched aOG (red curves), after sitting for 1 day (solid curves) or 7 days (dashed curves).

3.3 Comparing WSBA to radiocarbon sample cleaning protocols

In this work, we apply a water/sonication-base-acid (WSBA) treatment, which includes sonication during the water treatment, in order to separate a mixture of graphite, GO, and OD. This mixture is a simplistic model system that mimics the types of graphenic carbon materials that could be present in fossilized charcoal. This is the first time that graphenic carbon chemistry[10,17] been applied rationally to the separation of graphite-based materials related to radiocarbon dating applications.

We are not the first to use water treatments to separate charcoal from other carbonaceous material. In an earlier study, others found that significant weight loss can occur after water treatment of fossil charcoal.[2] They attributed the weight loss to removal of poorly preserved (oxidized) graphite, citing earlier work that suggested that fossil charcoal can be oxidized during weathering to produce carboxyl groups.[1,18] These earlier studies also suggested the possibility of OD formation in archaeological samples, proposed in terms of "self-humification."[18] These studies from the radiocarbon literature[1,2,18] pre-date much of the GO and OD separation literature that informs our WSBA protocol.[10,12,17]

In broader context, the reason that our experiments, and an explicit link between GO/OD literature and ABA literature, are important, is that they introduce informed strategies to capture and separate GO and OD from graphite. We are the first to propose this. This is significant because it opens the door for new experiments that could test the viability of using GO or OD as a material for radiocarbon dating. In principle, the oxidation processes that produce GO and OD from graphitic materials would not alter a specimen's original (datable) carbon. However, this idea has not been broached in the radiocarbon dating literature.

View Article Online
DOI: 10.1039/C9AY00046A

The current norm is that oxidized graphite should be removed before dating. For example, one modification of the ABA procedure is ABOx, wherein an oxidation process (based on $K_2Cr_2O_7$ and H_2SO_4) replaces the last acid (HCl) treatment in the usual ABA protocol, in order to remove oxidizable carbon before dating.[3,7]

Although it is logical that graphite would remain the preferred material for radiocarbon dating, some samples disintegrate dramatically after base (NaOH) washes during the standard ABA treatment.[2] For such poorly preserved samples wherein severe graphite oxidation is suspected, our WSBA protocol could be helpful for capturing additional graphenic carbon material, in the form of GO and/or OD. A substantial number of future experiments would be necessary to explore the conditions under which our WSBA treatment could help extract graphite-based materials that produce reliable radiocarbon dates.

One of the main operational differences between our WSBA separation procedure and other ABA-based cleaning procedures for datable radiocarbon materials is our use of sonication (Step 1 in Table 1). We explored a range of different experimental conditions to determine that filtration of suspensions (pH 5-8) and/or centrifugation (2000-8500 rpm, 1-15 minutes) on their own are not effective for separating graphite flakes from aOG. We found that the most effective method was to centrifuge (8500 rpm for 10 minutes) when the aqueous solution was strongly alkaline (pH 11), followed by filtering (8 μm pore size).

As described above, sonication is known to break aOG into smaller pieces more easily than graphite.[23–27] Optical microscopy images of our samples before and after sonication confirm that this holds true in our experiments (Figure 6). We note that these representative images do not give truly comprehensive information about the distribution of sizes within the full sample, but they do provide evidence that sonication reduces the particle sizes of aOG well below the pore size of our filter paper (8 μm diameter, $\sim$60 μm^2 cross-sectional area). For example, statistical analyses of particle sizes shown in Figure 6 indicate that sonication reduces the median particle area of graphite from $\sim$110 μm^2 to $\sim$80 μm^2, and reduces the median particle are of aOG from $\sim$110 μm^2 to $\sim$10 μm^2. This illustrates why it is feasible to separate the larger graphite pieces from the smaller aOG pieces using filtration. Based on our FTIR data (Figure 2), filtration-based size separation is very effective on our simplistic test mixture.

However, applying this method successfully to archaeological samples would likely be much more challenging. Factors such as oxidation method, reaction time, oxidants, pH, and sonication are known to affect the sizes of aOG particles[41–45], ranging from less than 1 μm to greater than 200 μm.[26,38,46,47] The stability and dispersibility of aOG in water are strongly associated with the lateral size of aOG and C-O content, and some studies have correlated zeta potential (effective surface charge) data with the suspension behaviours of aOG.[27] Thus, since any oxidation within an archaeological charcoal sample will undoubtedly occur in a very different manner from the harsh chemical oxidation that we used in our simplistic test model, the sonication step would likely have different effects on any given archaeological sample.

It is also worth noting that cleaning procedures for radiocarbon dating samples must be designed to avoid introducing different sources of carbon into the specimen. For example, samples are never handled with bare hands, and all stages of the cleaning involve aqueous treatments (to avoid contact with organic solvents). In the case of the WSBA procedure outlined here, we use carbon-based filter paper at two different stages (Steps 2 and 5 in Table 1). If future studies indicate a need to avoid contact with filter paper, we note that others have used a range of methods to isolate aOG particles based on size differences, including centrifugation, magnetic stirring, density gradient ultracentrifugation, and electrophoresis.[47–49]

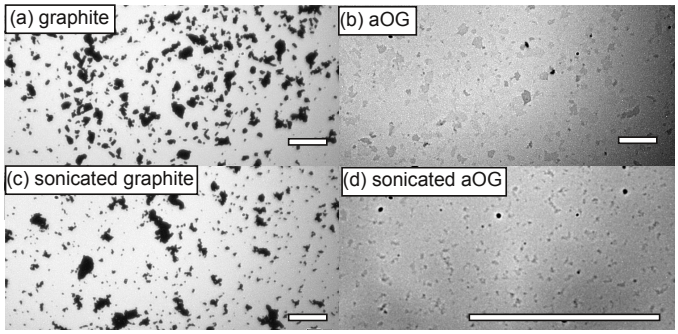

Fig. 6 Representative optical microscopy images of (a) graphite, (b) aOG, (c) sonicated graphite, and (d) sonicated aOG. The opaque graphite particles (a,c) show greater contrast than the optically transparent aOG (b,d). Scale bars represent 100 μm in all images; in (d), the image is magnified to show particle outlines more clearly.

4 Conclusions

In this work, we show synergies between (1) the chemistry involved in removing graphenic oxide (GO) and oxidative debris (OD) from oxidized graphenic carbon materials, and (2) the chemistry involved in ABA cleaning of graphenic carbon materials used for radiocarbon dating. Drawing on literature from the subfields of GO chemistry and radiocarbon dating, we introduce a different cleaning sequence of water/sonication-base-acid (WSBA) that is designed to separate graphite from GO and OD. Furthermore, we demonstrate that the relative proportions of OD and aOG – independent of any humic substances – can affect the ability of oxidized graphite to be suspended in water, which can effect the efficiency of the separation procedures we describe. In principle, this could be used to fine tune separation procedures during sample cleaning for radiocarbon sample preparation. Finally, we use the chemistry of OD to explain why WSBA could be more advantageous than traditional ABA cleaning procedures in some situations, such as the case when water and base treatments diminish the quantity of poorly preserved (oxidized) graphite that could be recovered after a standard ABA cleaning treatment. Looking forward, it is interesting to speculate whether GO and OD could be viable materials for radiocarbon dating, if extracted from archaeological charcoal samples.

5 Acknowledgements

Thanks to Bob Helleur for charcoal samples. KMP thanks the NSERC (Canada) Discovery Grant program for funding.

View Article Online
DOI: 10.1039/C9AY00046A

References

1 D. Alon, G. Mintz, I. Cohen, S. Weiner and E. Boaretto, *Radiocarbon*, 2002, **44**, 1–11.

2 N. R. Rebollo, I. Cohen-Ofri, R. Popovitz-Biro, O. Bar-Yosef, L. Meignen, P. Goldberg, S. Weiner and E. Boaretto, *Radiocarbon*, 2008, **50**, 289–307.

3 M. I. Bird, V. Levchenko, P. L. Ascough, W. Meredith, C. M. Wurster, A. Williams, E. L. Tilston, C. E. Snape and D. C. Apperley, *Quat. Geochronol.*, 2014, **22**, 25–32.

4 E. A. Olson and W. S. Broecker, *Transactions of the New York Academy of Sciences*, 1958, **20**, 593–604.

5 E. Bouleghlimat, P. R. Davies, R. J. Davies, R. Howarth, J. Kulhavy and D. J. Morgan, *Carbon*, 2013, **61**, 124–133.

6 F. Kang, Y. Leng, T. Y. Zhang and B. Li, *Carbon*, 1998, **36**, 383–390.

7 M. I. Bird, L. K. Ayliffe, L. K. Fifield, C. S. M. Turney, R. G. Cresswell, T. T. Barrows and B. David, *Radiocarbon*, 1999, **41**, 127–140.

8 P. L. Ascough, M. I. Bird, W. Meredith, R. E. Wood, C. E. Snape, F. Brock, T. F. G. Higham, D. J. Large and D. C. Apperley, *Radiocarbon*, 2010, **52**, 1336–1350.

9 S. Eigler, M. Enzelberger-Heim, S. Grimm, P. Hofmann, W. Kroener, A. Geworski, C. Dotzer, M. Rokert, J. Xiao, C. Papp, O. Lytken, H. P. Steinruck, P. Muller and A. Hirsch, *Adv. Mater.*, 2013, **25**, 3583–3587.

10 J. P. Rourke, P. A. Pandey, J. J. Moore, M. Bates, I. A. Kinloch, R. J. Young and N. R. Wilson, *Angew. Chem.*, 2011, **50**, 3173–3177.

11 T. Szabo, E. Tombacz, E. Illes and I. Dekany, *Carbon*, 2006, **44**, 537–545.

12 A. M. Dimiev, L. B. Alemany and J. M. Tour, *ACS Nano*, 2013, **7**, 576–588.

13 A. Bianco, H.-M. Cheng, T. Enoki, Y. Gogotsi, R. H. Hunt, N. Koratkar, T. Kyotani, M. Monthioux, C. R. Park, J. M. D. Tascon and J. Zhang, *Carbon*, 2013, **65**, 1–6.

14 W. S. Hummers and R. E. Offeman, *J. Am. Chem. Soc.*, 1958, **80**, 1339–1339.

15 D. C. Marcano, D. V. Kosynkin, J. M. Berlin, A. Sinitskii, Z. Sun, A. Slesarev, L. B. Alemany, W. Lu and J. M. Tour, *ACS Nano*, 2010, **4**, 4806–4814.

16 A. M. Dimiev and J. M. Tour, *ACS Nano*, 2014, **8**, 3060–3068.

17 H. R. Thomas, S. P. Day, W. E. Woodruff, C. Valles, R. J. Young, I. A. Kinloch, G. W. Morley, J. V. Hanna, N. R. Wilson and J. P. Rourke, *Chem. Mater.*, 2013, **25**, 3580–3588.

18 I. Cohen-Ofri, L. Weiner, E. Boaretto, G. Mintz and S. Weiner, *J. Archaeol. Sci.*, 2006, **33**, 428–439.

19 Z. Wang, M. D. Shirley, S. T. Meikle, R. L. Whitby and S. V. Mikhalovsky, *Carbon*, 2009, **47**, 73–79.

20 J. Chen, B. Yao, C. Li and G. Shi, *Carbon*, 2013, **64**, 225–229.

21 M. Rosillo-Lopez and C. G. Salzmann, *Carbon*, 2016, **106**, 56–63.

22 J. Schindelin, I. Arganda-Carreras and E. Frise, *Nature Meth.*, 2012, **9**, 676–682.

23 A. Ciesielski and P. Samori, *Chem. Soc. Rev.*, 2014, **43**, 381–398.

24 S. Ye and J. Feng, *RSC Advances*, 2016, **6**, 39681–39687.

25 Z.-S. Wu, W. Ren, L. Gao, B. Liu, J. Zhao and H.-M. Cheng, *Nano Research*, 2010, **3**, 16–22.

26 A. K. Swain, D. Li and D. Bahadur, *Carbon*, 2013, **57**, 346–356.

27 J. Kim, L. J. Cote, F. Kim, W. Yuan, K. R. Shull and J. Huang, *J. Am. Chem. Soc.*, 2010, **132**, 8180–8186.

28 R. Gu, W. Z. Xu and P. A. Charpentier, *J. Polym. Sci. A*, 2013, **51**, 3941–3949.

29 S. Peng, X. Fan, S. Li and J. Zhang, *J. Chil. Chem. Soc.*, 2013, **58**, 2213–2217.

30 A. Dimiev, D. V. Kosynkin, L. B. Alemany, P. Chaguine and J. M. Tour, *J. Am. Chem. Soc.*, 2012, **134**, 2815–2822.

31 H. R. Thomas, C. Valles, R. J. Young, I. A. Kinloch, N. R. Wilson and J. P. Rourke, *J. Mater. Chem. C*, 2013, **1**, 338–342.

32 R. A. Meyers and J. Coates, *Interpretation of Infrared Spectra, A Practical Approach*, New York, NY (USA) Wiley, 2000.

33 A. F. Faria, D. S. T. Martinez, A. C. M. Moraes, M. E. H. Maia da Costa, E. B. Barros, A. G. Souza Filho, A. J. Paula and O. L. Alves, *Chem. Mater.*, 2012, **24**, 4080–4087.

34 C. Monteserin, M. Blanco, E. Aranzabe, A. Aranzabe, J. Laza, A. Larranaga-Varga and J. Vilas, *Polymers*, 2017, **9**, 1–16.

35 Y. Li, H. Liu, X.-q. Liu, S. Li, L. Wang, N. Ma and D. Qiu, *Langmuir*, 2016, **32**, 8641–8649.

36 A. Bonanni, A. Ambrosi, C. K. Chua and M. Pumera, *ACS Nano*, 2014, **8**, 4197–4204.

37 R. Verdejo, S. Lamoriniere, B. Cottam, A. Bismarck and M. Shaffer, *ChemComm*, 2007.

38 J. Chen, Y. Li, L. Huang, N. Jia, C. Li and G. Shi, *Adv. Mater.*, 2015, **27**, 3654–3660.

39 W. Zhang, X. Zou, H. Li, J. Hou, J. Zhao, J. Lan, B. Feng and S. Liu, *RSC Adv.*, 2015, **5**, 146–152.

40 T. Szabo, O. Berkesi, P. Forgo, K. Josepovits, Y. Sanakis, D. Petridis and I. Dekany, *Chem. Mater.*, 2006, **18**, 2740–2749.

41 J. Zhao, S. Pei, W. Ren, L. Gao and H.-M. Cheng, *ACS Nano*, 2010, **4**, 5245–5252.

42 X. Zhou and Z. Liu, *ChemComm*, 2010, **46**, 2611–2613.

43 X. Wang, H. Bai and G. Shi, *J. Am. Chem. Soc.*, 2011, **133**, 6338–6342.

44 C. Y. Su, Y. Xu, W. Zhang, J. Zhao, X. Tang, C. H. Tsai and L. J. Li, *Chem. Mater.*, 2009, **21**, 5674–5680.

45 S. Pan and I. A. Aksay, *ACS Nano*, 2011, **5**, 4073–4083.

46 K. E. Lee, J. E. Kim, U. N. Maiti, J. Lim, J. O. Hwang, J. Shim, J. J. Oh, T. Yun and S. O. Kim, *ACS Nano*, 2014, **8**, 9073–9080.

47 H. Geng, B. Yao, J. Zhou, K. Liu, G. Bai, W. Li, Y. Song, G. Shi, M. Doi and J. Wang, *J. Am. Chem. Soc.*, 2017, **139**, 12517–12523.

48 Y. Liu, D. Zhang, S. Pang, Y. Liu and Y. Shang, *J. Sep. Sci.*, 2015, **38**, 157–163.

49 S. Li, F. Zhu, F. Meng, H. Li, L. Wang, J. Zhao, Q. Yue, J. Liu and J. Jia, *J. Electroanal. Chem.*, 2013, **703**, 135–145.

View Article Online
DOI: 10.1039/C9AY00046A

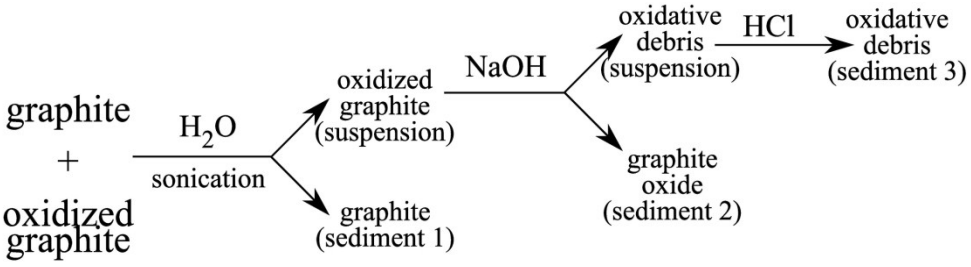

Our protocol has potential applications for separating graphite oxide from graphite and oxidative debris for radiocarbon dating purposes.

203x63mm (300 x 300 DPI)